UC Irvine

UC Irvine Previously Published Works

Title

Ito Channels Are Octomeric Complexes with Four Subunits of Each Kv4.2 and K+ Channel-interacting Protein 2*

Permalink

https://escholarship.org/uc/item/0qd1d0hj

Journal

Journal of Biological Chemistry, 279(7)

ISSN

0021-9258

Authors

Kim, Leo A
Furst, Johannes
Butler, Margaret H
et al.

Publication Date

2004-02-01

DOI

10.1074/jbc.m311332200

Copyright Information

This work is made available under the terms of a Creative Commons Attribution License, availalbe at https://creativecommons.org/licenses/by/4.0/

Peer reviewed

eScholarship.org Powered by the California Digital Library
University of California

THE JOURNAL OF BIOLOGICAL CHEMISTRY
Vol. 279, No. 7, Issue of February 13, pp. 5549–5554, 2004
© 2004 by The American Society for Biochemistry and Molecular Biology, Inc.
Printed in U.S.A.

I_{to} Channels Are Octomeric Complexes with Four Subunits of Each Kv4.2 and K^+ Channel-interacting Protein 2*

Received for publication, October 15, 2003, and in revised form, November 11, 2003
Published, JBC Papers in Press, November 17, 2003, DOI 10.1074/jbc.M311332200

Leo A. Kim‡§, Johannes Furst¶‖, Margaret H. Butler‡, Shuhua Xu‡, Nikolaus Grigorieff¶, and Steve A. N. Goldstein‡**

From the ‡Departments of Pediatrics and Cellular and Molecular Physiology, Boyer Center for Molecular Medicine, Yale University School of Medicine, New Haven, Connecticut 06536 and the ¶Howard Hughes Medical Institute and Department of Biochemistry, Rosenstiel Basic Medical Sciences Research Center, Brandeis University, Waltham, Massachusetts 02454

Mammalian voltage-gated K^+ channels are assemblies of pore-forming α-subunits and modulating β-subunits. To operate correctly, Kv4 α-subunits in the heart and central nervous system require recently identified β-subunits of the neuronal calcium sensing protein family called K^+ channel-interacting proteins (KChIPs). Here, Kv4.2·KChIP2 channels are purified, integrity of isolated complexes confirmed, molar ratio of the subunits determined, and subunit valence established. A complex has 4 subunits of each type, a stoichiometry expected for other channels employing neuronal calcium sensing β-subunits.

In muscles and nerves, Kv4 (Shal family) α-subunits assemble with K^+ channel-interacting proteins (KChIPs)[1] β-subunits to create mixed complexes with unique attributes and functions (1–7). Thus, Kv4 channels produce rapidly activating and inactivating currents, such as I_{to}, which mediates the early repolarization phase of the cardiac action potential (8–11), and I_A, to regulate action potential propagation and frequency in neurons (12–14). KChIP subunits 1–4 enjoy differential tissue distribution, splice variation and carry EF-hand motifs as do other neuronal calcium sensing peptides (including frequenin, recoverin, guanylyl cyclase activating protein, and the visinin-like proteins visinin-like proteins 1–3, neurocalcin, and hippocalcin) (15); the roles of visinin-like proteins are now emerging.

KChIPs (and frequenin) (16, 17) have been shown to assemble with Kv4 subunits in stable fashion leading to increased current density due to enhanced surface expression, activation at more hyperpolarized potentials, slowed inactivation, and speeded recovery from inactivation (1, 2, 16). These β-subunits permit kinase regulation (18), control trafficking, and alter surface half-life (6). So, the increase in I_{to} across canine cardiac ventricular wall (from endo- to epicardium) reflects a parallel gradient in KChIP2 expression (3), and transgenic mice devoid of KChIP2 have no measurable I_{to}, a prolonged action potential, and susceptibility to ventricular arrhythmia (4).

Functional and structural studies of α-subunits demonstrate that K^+ channel conduction pores are formed by assembly of 4 pore loops about a central axis (19). Conversely, K^+ channel accessory subunits vary in their nature (soluble, peripheral, or membrane-spanning) and number per complex (20). To explore the structural basis for KChIP function, the stoichiometry of Kv4.2·KChIP2 channels was determined using a stepwise strategy: significant amounts of intact, functional Kv4.2·KChIP2 complexes were produced and isolated; functional and structural integrity of the purified material was confirmed by a toxin binding assay; and, thereafter, subunit valence was established by gradient centrifugation and direct amino acid analysis.

MATERIALS AND METHODS

Molecular Biology—Human Kv4.2 and KChIP2 were expressed in pRAT, a dual purpose vector with a cytomegalovirus promoter for mammalian expression and a T7 promoter for cRNA synthesis. Charybdotoxin (CTX)-sensitive Kv4.2 (Kv4.2*) was produced by plaque-forming unit-based mutation (Stratagene, La Jolla, CA); the pore segment containing mutations was isolated with NruI and BamHI and replaced into a wild-type human Kv4.2 backbone. The 1D4 epitope was introduced by creating an Mlu1 site in place of the termination codon and inserting a nucleotide compatible to Mlu1 and BglII encoding a linker and the epitope (RVPDGDPDETSQVAPAX). cRNA was synthesized after linearization with NotI using an mMessage mMachine kit (Ambion, Austin, TX). cRNAs were quantified by spectroscopy and gel electrophoresis. The gene variants used in this study were human Kv4.2 (accession number AH009258), KChIP2 (accession number AF199598), and Kv1.3 (accession number NM_002232).

Electrophysiology and Data Analysis—Oocytes from *Xenopus laevis* frogs were defolliculated by collagenase and injected with 0.2 ng of Kv4.2 or Kv4.2* and 0.4 ng of KChIP2 cRNA. For CTX block studies less cRNA was injected for mixed complexes so macroscopic current was like that for α-subunits alone. Currents were studied at 12–24 h. Whole-cell currents were measured by two electrode voltage clamp (Geneclamp 500, Axon Instruments, Union City, CA). Electrodes were filled with 3 M KCl and had resistance of 0.1–1.2 MΩ. Data were sampled at 1 kHz. Data recording was performed using Clampex v8.0 and assessed with Clampfit v8.0, Excel, and Origin 6.0. All experiments were performed at room temperature. Standard bath solution was ND-96: 96 mM NaCl, 2 mM KCl, 1 mM $MgCl_2$, 1.8 mM $CaCl_2$, 5 mM HEPES/NaOH, pH 7.5) and supplemented with 0.1% bovine serum albumin for CTX studies. CTX binding kinetics were examined with voltage pulses to 40 mV for 500 ms from a resting membrane voltage of −80 mV repeated every 20 s. Current-voltage curves were evoked by depolarizing from a holding potential of −100 mV to test potentials of −80 to 70 mV with 10 mV steps lasting 500 ms every 5 s. Steady state inactivation was examined from a holding potential of −100 mV with test pulses from −120 to 10 mV held for 2.5 s with a second pulse at 40 mV to measure currents that were not inactivated. Recovery from inactivation was measured by

* This work was supported by grants from the National Institutes of Health (to S. A. N. G. and N. G.). The costs of publication of this article were defrayed in part by the payment of page charges. This article must therefore be hereby marked "*advertisement*" in accordance with 18 U.S.C. Section 1734 solely to indicate this fact.

§ Participant in the Medical Scientist Training Program (GM07205).

‖ Supported by a fellowship from the Max Kade Foundation. Present address: Institute of Physiology, University of Innsbruck, Fritz-Pregl-Str. 3, A-6020 Innsbruck, Austria.

** A Doris Duke Distinguished Clinical Scholar. To whom correspondence should be addressed. E-mail: steve.goldstein@yale.edu.

[1] The abbreviations used are: KChIP, K^+ channel-interacting protein; CTX, charybdotoxin; Kv4.2*, a CTX-sensitive Kv4.2 channel variant; 1D4, an 8 residue C-terminal epitope; CHAPS, 3-[(3-cholamidopropyl)dimethylammonio]-1-propanesulfonic acid.

driving channels to an inactivated state at 40 mV, hyperpolarizing to −100 mV, and then applying a second pulse to 40 mV for various intervals (increments of 5 and 50 ms). Inactivation was fit to a double exponential equation. Recovery from inactivation was fit to a single exponential. Activation $V_{0.5}$ and V_s were calculated by fitting the conductance-voltage relationship to a Boltzmann function. Similarly, inactivation $V_{0.5}$ and V_s were calculated by fitting the normalized current-voltage relationship to a Boltzmann function.

Expression and Purification with COS7 Cells—Kv4.2* was co-expressed with KChIP2 in COS7 cells using LipofectAMINE 2000 (Invitrogen, Carlsbad, CA) and 2.5 and 5 μg cDNA/plate, respectively. 10–25 100 mm plates were harvested 2 days after transfection and solubilized for 1 h at 4 °C in lysis buffer containing 2.5% CHAPS, 100 mM NaCl, 40 mM KCl, 1.0 mg/ml *Escherichia coli* lipid, 1 mM dithiothreitol, 0.2 mM leupeptin/pepstatin, 1 mM EDTA, 20 mM HEPES-KOH, pH 7.4, and 10% glycerol with Complete protease inhibitors (Roche Applied Science). Soluble material (SM) was collected after centrifugation at 100,000 × *g* for 45 min. The extract was incubated with anti-1D4-coated beads for 2 h at 4 °C with agitation often between New Haven, CT, and Waltham, MA (Honda Civic 1999). The column was washed with 50 ml of wash buffer containing 0.7% CHAPS, 300 mM NaCl, 40 mM KCl, 0.01 mM leupeptin/pepstatin, 1 mM EDTA, 20 mM HEPES-KOH, pH 7.4 with Complete protease inhibitors (Roche Applied Science). Protein was then eluted (E) in wash buffer with 100 mM NaCl and 0.2 mg/ml 1D4 peptide (Yale University Keck Facility). 1D4 monoclonal antibody was purchased (NCCC, Minneapolis MN) and coupled to beads as before (21). KChIP2 antibodies were a generous gift (J. Trimmer, University of California, Davis).

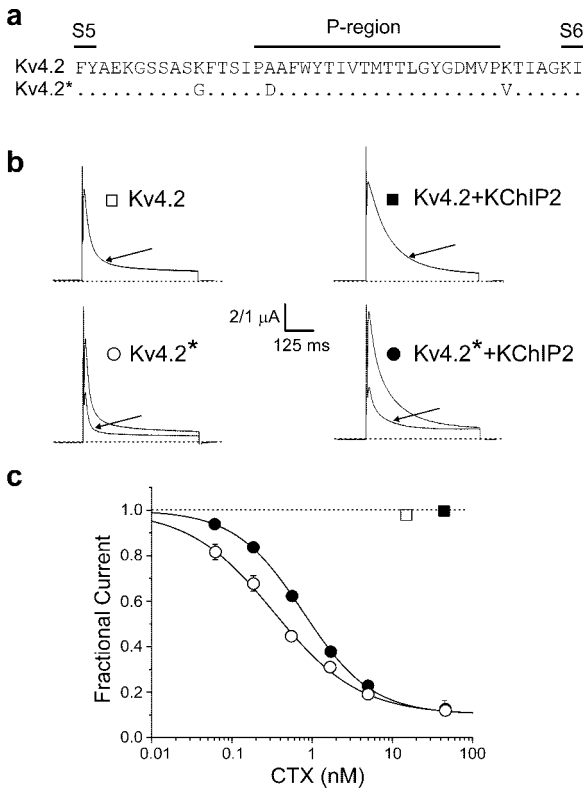

FIG. 1. **A CTX-sensitive variant of Kv4.2.** *a*, alignment of the pore loop region of human Kv4.2 (residues 343–385 shown) and the toxin-sensitive mutant (Kv4.2*); changes reproduce residues in Kv1.3. *b*, wild-type Kv4.2 (*open square*) and Kv4.2·KChIP2 channels (*filled square*) are insensitive to CTX (*arrows*), 15 and 45 nM applied, respectively. Kv4.2* (*open circle*) and Kv4.2*·KChIP2 channels (*filled circles*) are blocked by 1.67 nM CTX (*arrows*). Channels expressed in oocytes studied by two-electrode voltage clamp with depolarization from −100 to 40 mV for 500 ms every 20 s (see "Materials and Methods"). *c*, CTX block of channels formed by Kv4.2* (*open circles*) and Kv4.2*·KChIP2 (*filled circles*). Data represents unblocked fractional current as a function of CTX concentration and is fit to: $f_u = (1 + ([CTX]/K_i)^h)^{-1}$. Fits yield $K_i = 0.35 \pm 0.04$ and 0.76 ± 0.03, with coefficients h = 0.89 and 1.02, respectively. Each point is mean ± S.E. for 3–10 oocytes.

Whole-cell CTX Binding—^{3}H-CTX binding to cells was performed as described previously (22). Briefly, cell samples were divided into control and test groups. Control assessed nonspecific binding of ^{3}H-CTX (36 nM) that took place in the presence of 1 μM non-radioactive CTX. Test groups measured total ^{3}H-CTX binding and specific binding was determined by subtracting the nonspecific from the total binding. All steps were performed at 4 °C. Cells were exposed to ^{3}H-CTX in binding buffer (20 mM KCl, 10 mM NaPi, 100 mM sucrose, and 1 mg/ml bovine serum albumin) for 30 min, collected by centrifugation for 1 min at 3,000 rpm, and the supernatant was removed. The cell pellet was washed in 100 μl binding buffer, centrifuged, and after removal of supernatant, suspended in 100 μl of buffer, transferred to a scintillation vial with 10 ml of scintillation fluid (SafeScint, American Bioanalytical, Natick, MA) for liquid scintillation counting.

CTX Binding to Purified Complexes—A 50 μl elution of purified material was exposed to 36 nM ^{3}H-CTX with or without 1 μM unlabelled CTX. As above, the two samples were used to assess nonspecific and total binding of ^{3}H-CTX. Binding was performed at 4 °C for 30 min, 8 h, 16 h, or 24 h, after which unbound toxin was removed with an Amicon Centricon 100 (Millipore, Billerica, MA) by centrifugation for 10 s at 9,000 rpm and a wash with 20 μl wash buffer with only 100 mM NaCl by centrifugation. The filter was then placed in a liquid scintillation vial and studied in a scintillation counter as above. The dose-titration assay was performed in a similar manner with 25 μl aliquots of purified channel complex. 0, 0.45, 1.33, 4, 12, or 36 nM ^{3}H-CTX was applied to a control and test sample for 30 min at 4 °C and processed as above.

Glycerol Gradient Analysis—Kv4.2*·KChIP2 protein complex (0.5 ml, ~2 μg, E2–4) was layered on a 12 ml 10–40% (w/v) linear glycerol gradient containing 0.7% CHAPS, 100 mM NaCl, 40 mM KCl, 1 mM EDTA, 20 mM HEPES-KOH, pH 7.4, and Complete protease inhibitors (Roche Applied Science). A parallel gradient was layered with 20 μg of each of the following molecular mass markers (Amersham Biosciences); chymotrypsinogen (25 kDa), albumin (67 kDa), aldolase (158 kDa), catalase (232 kDa), and ferritin (440 kDa). Gradients were centrifuged for 15 h at 35,000 rpm and 4 °C using an SW41 rotor (Beckman, Fullerton, CA). 1-ml fractions were collected by upward displacement. Proteins were precipitated with 5 volumes acetone at −20 °C for analysis.

Amino Acid Analysis—After SDS-PAGE and staining with Coomas-

TABLE I

Channel gating parameters for Kv4.2 and Kv4.2 channels with and without KChIP2*

Parameters for Kv4.2 and Kv4.2* expressed alone or with KChIP2 from measurements by two electrode voltage clamp using oocytes as described under "Materials and Methods." $V_{0.5}$ and V_s were calculated by fitting the conductance-voltage and normalized current-voltage relationships, respectively, to a Boltzmann function. Inactivation kinetics were fit to a double exponential function. Recovery kinetics were fit to a single exponential.

	Kv4.2	Kv4.2+KChIP2	Kv4.2*	Kv4.2*+KChIP2
Activation $V_{0.5}$ (mV)	−24.3 ± 0.6	−26.8 ± 0.9	−28.9 ± 1.0	−30.2 ± 0.9
Activation V_s (mV)	13.7 ± 0.3	10.3 ± 0.2	12.0 ± 0.3	8.5 ± 0.1
V_{peak} at 40 mV (μA)	1.5 ± 0.1	4.9 ± 0.4	2.2 ± 0.3	4.9 ± 0.6
Inactivation $V_{0.5}$ (mV)	−62.2 ± 0.8	−50.3 ± 1.0	−58.6 ± 0.6	−52.5 ± 0.4
Inactivation V_s (mV)	6.1 ± 0.2	3.50 ± 0.03	6.6 ± 0.2	3.20 ± 0.02
Inactivation τ_{slow} (ms)	204 ± 20	197 ± 15	140 ± 21	172 ± 9
Inactivation τ_{fast} (ms)	30.5 ± 4.2	62.4 ± 4.7	21.8 ± 2.0	22.4 ± 3.3
$A_{slow}/(A_{slow}+A_{fast})$	0.17	0.48	0.20	0.48
$A_{fast}/(A_{slow}+A_{fast})$	0.83	0.52	0.80	0.52
Recovery τ_{rec}	192 ± 8	19.3 ± 0.6	221 ± 8	24.5 ± 1.5
n (no. of oocytes)	5	5–8	5–6	5–11

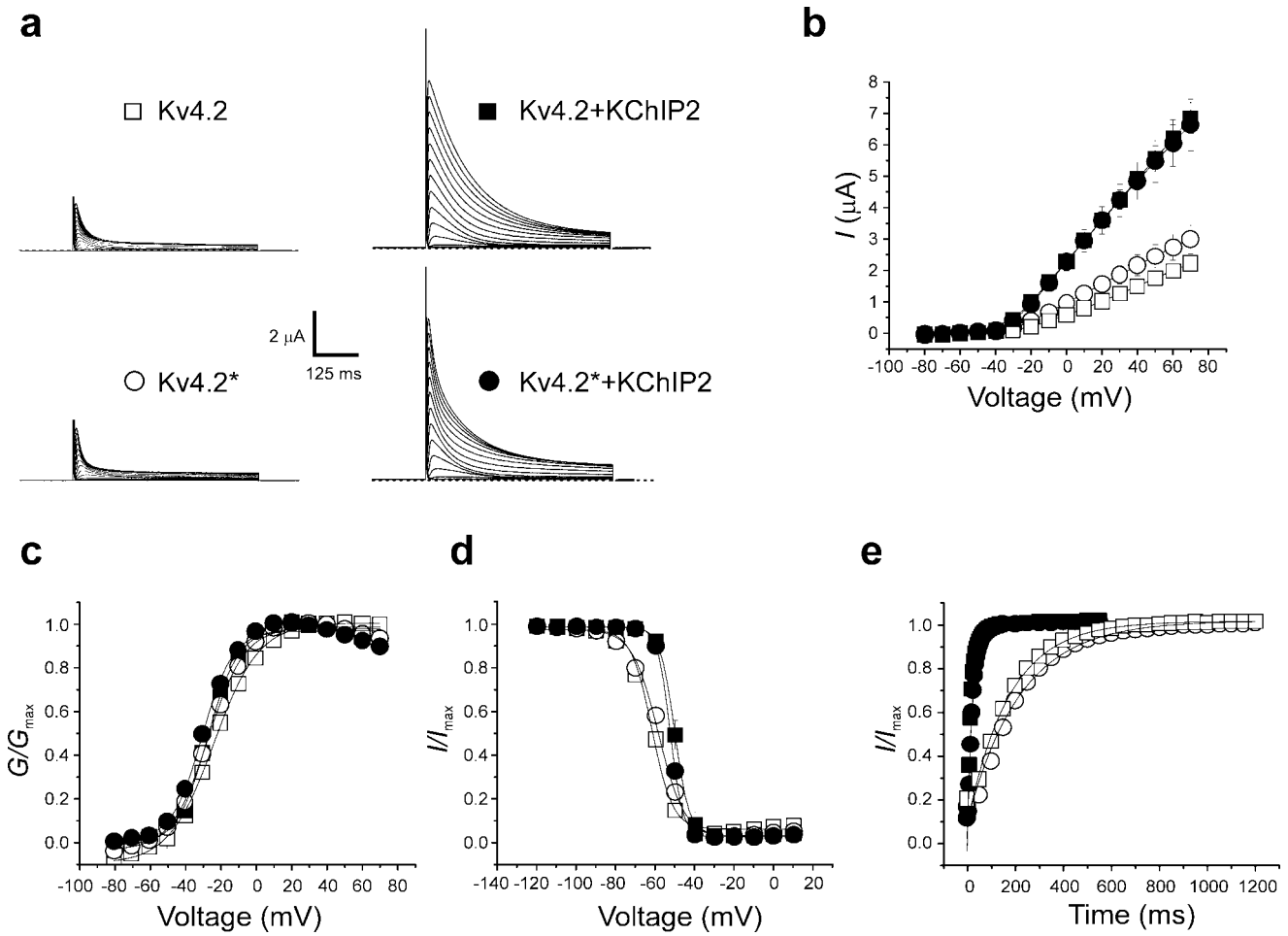

FIG. 2. **KChIP2 has similar effects on Kv4.2 and the CTX-sensitive variant Kv4.2*.** Channels expressed in oocytes and studied by two-electrode voltage clamp (see "Materials and Methods"); determined gating parameters in Table I. Symbols for each channel type are as in Fig. 1*b*: wild-type Kv4.2 (*open square*); Kv4.2·KChIP2 channels (*filled square*); Kv4.2* (*open circle*) and Kv4.2*·KChIP2 channels (*filled circles*). *a*, currents evoked by depolarizing from a holding potential of −100 mV to test potentials of −80 to 70 mV in 10 mV steps lasting 500 ms every 5 s. *b*, current-voltage relationship shows 2–3-fold increase in current density with KChIP2. *c*, conductance-voltage relationship shows hyperpolarizing shift with KChIP2. *d*, inactivation-voltage relationship shows right shift in steady state inactivation with KChIP2. *e*, recovery from inactivation reveals a ~10-fold increase in the rate of recovery with KChIP2.

sie Brilliant Blue, bands corresponding to Kv4.2* and KChIP2 and a blank portion of the gel were excised with a sterile scalpel. Samples were hydrolyzed in 6 N HCl and 0.2% phenol for 16 h at 115 °C with 2 nmol norleucine/100 μl HCl as an internal standard. After hydrolysis, amino acids were quantified on a Beckman 7300 Amino Acid Analyzer via ion-exchange and post-column ninhydrin detection (Yale University Keck Facility). After quantification, some amino acids are not analyzed due to intrinsic limitations of the method: these include His, which co-elutes with Tris in the SDS-PAGE buffer, Gly, which is in SDS-PAGE buffer, and Arg, which is variably obscured by ammonia in gel samples. Amino acids residues determined for the blank gel sample were subtracted from subunit samples to correct for background signal. 9–12 amino acids for each subunit were observed to be within 10% of predicted value in each trial and were studied: Asn, Asp, Thr, Gln, Glu, Pro, Ala, Val, Ile, Leu, Phe, and Lys.

RESULTS

First, a variant of human Kv4.2 α-subunits (Kv4.2*) was produced that maintained the functional attributes of wild-type but had two modifications, a pore binding site for the peptide toxin CTX and an 8 residue C-terminal epitope tag (1D4, ETSQVADA). The rationale for these embellishments was as follows. A single CTX molecule binds in the ion conduction pore of toxin-sensitive K^+ channels to occlude the permeation pathway only when 4 permissive α-subunits are assembled in correct fashion; as a result, small changes in pore (or toxin) structure are registered with great sensitivity as altered blockade (23–25). Thus, CTX and related toxins were used to locate the external aspect of the conduction pore (26), assess its dimensions (27, 28), count channels (22), and, as here, assess the integrity of purified channel protein (19). The 1D4 epitope allows purification of membrane proteins under mild conditions via monoclonal antibody binding and peptide elution (21).

The CTX-sensitive variant of Kv4.2 was produced by introduction of 3 mutations in the pore loop (Fig. 1*a*) chosen in an iterative fashion based on residues found to be important for high-affinity toxin binding in other K^+ channels (29, 30). Although wild-type Kv4.2 channels are insensitive to application of CTX, those with Kv4.2* α-subunits show half-maximal block (K_i) at 0.35 ± 0.04 nM (Fig. 1, *b* and *c*). Similarly, wild-type Kv4.2·KChIP2 channels are insensitive to toxin whereas those with Kv4.2* α-subunits showed K_i = 0.76 ± 0.03 nM (Fig. 1, *b* and *c*). As CTX is external and KChIP2 subunits are intracellular, the increase in K_i observed on KChIP2 incorporation was unexpected. Relaxation to equilibrium blockade upon acute toxin application revealed KChIP2 to have little effect on the toxin on-rate (K_{on} = 18.1 ± 1.4 μM^{-1} s^{-1} *versus* K_{on} = 24.5 ± 2.3 μM^{-1} s^{-1} with KChIP2, n = 8–10) but to destabilize bound toxin, increasing its off-rate ~3-fold (K_{off} = 8.0 ± 0.6 × 10^{-3} s^{-1} *versus* K_{off} = 22.9 ± 2.6 × 10^{-3} s^{-1}). This indicates small KChIP2-induced changes in the external pore of the closed channel (the predominant state in this protocol).

Despite modifications to confer CTX sensitivity and append

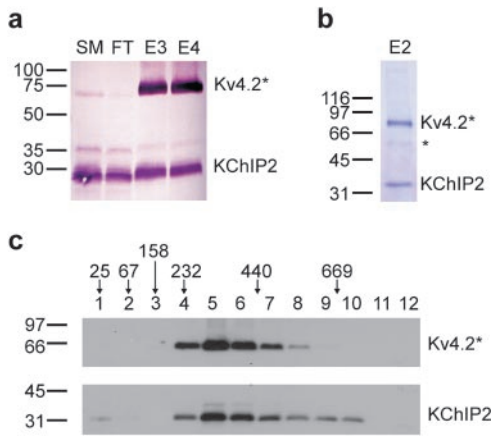

FIG. 3. **Purification of Kv4.2*·KChIP2 complexes and estimation of mass by glycerol gradient centrifugation.** *a*, purified Kv4.2*-KChIP2 channels separated by 10% SDS-PAGE, transferred to nitrocellulose, and probed with anti-1D4 and anti-KChIP2 antibodies. *SM*, soluble material from COS7 cell lysate. *FT*, flow through material that did not bind to the anti-1D4 antibody-coated beads. *E3* and *E4*, peptide elution fractions 3 and 4. *b*, E2 fraction separated by SDS-PAGE and stained with Coomassie Brilliant Blue. The bands corresponding to each subunit were excised and subjected to amino acid analysis (Table II). The *band* with a *star* is a minor contaminant (<1%) of 1D4 purifications (21). *c*, E2 fraction applied to a 10–40% glycerol gradient subjected to centrifugation and examined by 10% SDS-PAGE and Western blot analysis with anti-1D4 and anti-KChIP2 antibodies. Peak fractions for Kv4.2*·KChIP2 complexes are between markers at 232 and 440 kDa (catalase and ferritin, respectively).

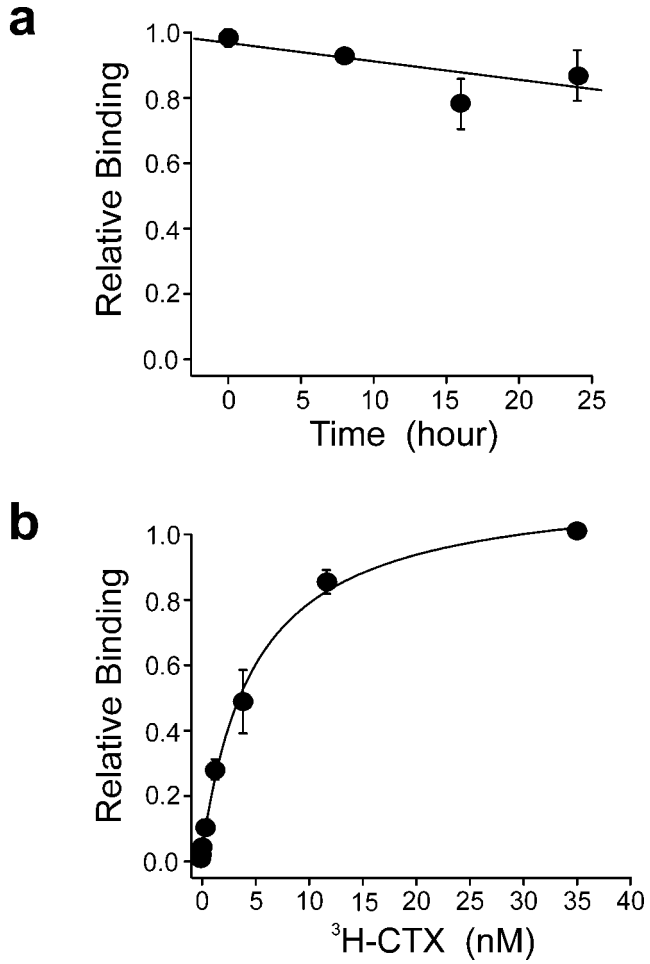

FIG. 4. **^{3}H-CTX binding reveals stability and integrity of purified Kv4.2*·KChIP2 complexes.** *a*, ^{3}H-CTX binding to Kv4.2*·KChIP2 complexes at various times after isolation: 30 min, 8 h, 16 h, and 24 h (n = 3), as in "Materials and Methods." *b*, ^{3}H-CTX binding to Kv4.2*·KChIP2 complexes with increasing ^{3}H-CTX (0, 0.45, 1.33, 4, 12, or 36 nM) and fit to a single-site function reveals K_d ~4.8 nM (n = 4), as in "Materials and Methods."

the epitope tag, channels with Kv4.2* behaved almost like those with wild-type subunits (Table I and Fig. 2). Kv4.2* channels are like wild-type in their voltage-dependence for half-maximal activation and half-maximal steady state inactivation. Although small differences in inactivation kinetics were observed for slow (τ_{slow}) and fast (τ_{fast}) time constants, these were without associated changes in their relative ratio, or rates of recovery from inactivation. Moreover, the archetypal effects of KChIP2 were unaltered by the α-subunit mutations. Thus, KChIP2 produced similar increases in current density and rates of recovery from inactivation with both wild type Kv4.2 and Kv4.2*, and similar decreases in rates of inactivation (due to increased contribution of the slow component) with expected small shifts in the voltage required to achieve half-maximal activation and half-maximal steady state inactivation.

Radioactive CTX (^{3}H-CTX) was synthesized as previously reported (22) and used first to monitor and optimize surface expression of channels on COS7 cells (see "Materials and Methods"). As expected based on measurement of channel currents, KChIP2 increased the absolute number of channels on the cells ~2.6-fold, from 1.6 ± 0.2 pmol/plate (n = 4) to 4.0 ± 0.2 pmol/plate (n = 11). Purification of Kv4.2*·KChIP2 complexes was achieved via the 1D4 epitope on Kv4.2* with anti-1D4 antibodies covalently bound to beads (Fig. 3). Thus, COS7 cells induced to transiently express Kv4.2* and KChIP2 at high levels were solubilized with the detergent CHAPS (2.5%), and complexes isolated by binding, washing with buffer, and elution with 1D4 peptide (see "Materials and Methods"). This led to co-purification of Kv4.2* and KChIP2 (Fig. 3, *a–c*). Western blot analysis revealed excess KChIP2 in soluble material (SM) and unbound flow though (FT) whereas Kv4.2*·KChIP2 channels were enriched in fractions collected by peptide elution (E) (Fig. 3*a*). Staining with Coomassie Blue confirmed the E2 fraction to be rich in the two channel subunits (Fig. 3*b*).

Purified material was subjected to centrifugation through a glycerol gradient and studied by Western blot analysis after SDS-PAGE to estimate the size of Kv4.2*·KChIP2 channels. The complex had a molecular mass between 232–440 kDa in trials with four separate preparations (Fig. 3*c*). Because Kv4.2* subunits carry no carbohydrate, each 642 residue protein has a predicted mass of ~72 kDa and each tetramer a mass of ~288 kDa (an underestimate due to detergent binding (21)). Because KChIP2 has 252 residues and a predicted mass of ~28 kDa this result argues that complexes contain between 1 and 6 KChIP2 subunits (~316–456 kDa). The predicted mass for an octameric complex with 4 Kv4.2* subunits and 4 KChIP2 subunits is 400 kDa.

To verify the stability and integrity of purified Kv4.2*·KChIP2 channels over time, binding of ^{3}H-CTX to isolated complexes was assessed. After 24 h at 4 °C, ~90% of the binding activity was retained (Fig. 4*a*). Indeed, despite residence in detergent rather than a lipid membrane, purified complexes bound ^{3}H-CTX with high affinity. Binding studies with four separate preparations Kv4.2*·KChIP2 were well fit to a single-site binding (Langmuir) isotherm with a K_d ~4.8 nM (Fig. 4*b*). Because CTX binding occurs with high affinity only when pores are properly assembled, the results provide direct evidence that the isolated complexes are a good approximation of the channels in plasma membranes and indicate their homogeneity because a single high affinity toxin site is apparent.

To accurately assess the subunit composition of purified Kv4.2*·KChIP2 complexes, the two subunits were separated by SDS-PAGE, identified by staining with Coomassie Brilliant

TABLE II
Moles of Kv4.2 and KChIP2 subunits in channel complexes*

Amino acids determined from Kv4.2* and KChIP2 bands excised from SDS-PAGE gels; 9–12 amino acids for each subunit in each study were within 10% of the predicted number and used individually to assess pmol of recovered subunit. Ratio is the molar ratio of pmol KChIP2 to Kv4.2* subunits.

Study	Kv4.2*	KChIP2	Ratio
	pmol	*pmol*	
1	3.00 ± 0.1	3.47 ± 0.1	1.15
2	10.3 ± 0.2	11.0 ± 0.2	1.06
3	11.3 ± 0.3	10.3 ± 0.2	0.91

Blue dye, and the bands excised from the gel for amino acid analysis by hydrolysis, ion-exchange chromatography, and ninhydrin detection (Table II). Because the amino acid sequences of Kv4.2* and KChIP2 were known, the expected and observed amino acid content of the bands could be compared and the moles of each subunit determined independently from 9–12 residues in each of 3 independent trials. The molar ratio of Kv4.2*:KChIP2 in purified complexes was 1:1 (Table II); similar results are noted in a companion report for channels with a KChIP2 variant and others with a Kv4.2* mutant.[2] Purified channels are shown to have 4 α-subunits because CTX binds with high affinity (Fig. 4). A 1:1 molar ratio therefore indicates that Kv4.2*·KChIP2 complexes contain 4 KChIP2 subunits.

DISCUSSION

Accessory β-subunits are a fundamental feature of K^+ channels that determine channel location, abundance, sensitivity to stimulation, and pharmacology *in vivo* (6, 20, 32). Here we demonstrate that regulatory KChIP2 subunits assemble with pore-forming Kv4.2 subunits in 4:4 complexes when over-expressed in tissue culture cells to produce voltage-gated K^+ channels like those in native cells (such as cardiac I_{to} (3, 4)). A 4:4 subunit arrangement appears to be the natural and stable valence for Kv4.2*·KChIP2 channels first because it was found with four separate large-scale preparations and second because KChIPs could not be separated from α-subunits without complete dissociation of the complexes to monomer form (not shown). KChIP2 increases trafficking to the surface, channel half-life, and detergent solubility of mixed complexes formed with Kv4.2 (6). This suggests why we could purify significant amounts of Kv4.2*·KChIP2 channels but did not succeed when Kv4.2* α-subunits were expressed alone (not shown). We expect KChIPs and related neuronal calcium sensing proteins (such as frequenin (16)) to assemble with other K^+ channel α-subunits with 4:4 stoichiometry to yield similar effects on stability, structure, and function.

A 4:4 subunit stoichiometry is also seen with the soluble intracellular regulator Kvβ2 in assemblies with the N-terminal segments of Kv1 α-subunits (33). Similarly, *KCNMB1*-encoded β-subunits (two span transmembrane proteins) and voltage- and calcium-gated BK α-subunits assemble with 4:4 valence (34, 35). The same subunit ratio is found with SUR β-subunits (bearing 17 predicted transmembrane segments) and Kir6.2 α-subunits (36–38). In contrast, just 2 *KCNE1*-encoded MinK β-subunits (peptides with a single transmembrane span) assemble with 4 KCNQ1 α-subunits to form cardiac I_{Ks} channels (39, 40); a 2:4 ratio is therefore expected for other channels with MinK-related peptides (MiRP1–4) (20). How many DPPX monomers (another single span β-subunit) assemble with Kv4 α-subunits (41) is yet to be determined.

In a companion study,[2] Kv4.2*·KChIP2 complexes purified by the strategy described here were found amenable to visualization by negative stain electron microscopy; demonstration here that isolated complexes maintain structural integrity and have 4:4 subunit valence allowed three-dimensional images of the channels to be reconstructed with a resolution of 21 Å. KChIP2 incorporation was found to create an $\sim 36 \times 115 \times 115$ Å, intracellular fenestrated rotunda: 4 peripheral columns that extend down from the membrane-embedded portion of the channel to enclose the central Kv4.2 "hanging gondola" (a platform held beneath the transmembrane conduction pore by 4 internal columns) (21, 31, 42, 43). To reach the pore from the cytosol, ions pass through one of four external fenestrae to enter the rotundal vestibule and then cross one of four internal windows in the gondola. The location of KChIP2 subunits in the structure is lateral to the gondola platform and does not overlap with the sub-platform locale for the Kvβ2 subunits apparent in crystal structures (33). It is as yet unknown whether a single channel complex can carry more than one type of accessory subunit and if subunit stoichiometry is thereby varied. These issues are under study by the methods described here.

Acknowledgments—We are grateful to J. Trimmer for anti-KChIP2 antibodies. National Cell Culture Center (NCCC) provided anti-1D4 antibodies. We thank R. Goldstein for help with the text and C. Miller for advice and help with synthesis of ^{3}H-CTX.

REFERENCES

1. An, W. F., Bowlby, M. R., Bett, M., Cao, J., Ling, H. P., Mendoza, G., Hinson, J. W., Mattsson, K. I., Strassle, B. W., Trimmer, J. S., and Rhodes, K. J. (2000) *Nature* **403,** 553–556
2. Bahring, R., Dannenberg, J., Peters, H. C., Leicher, T., Pongs, O., and Isbrandt, D. (2001) *J. Biol. Chem.* **276,** 23888–23894
3. Rosati, B., Pan, Z., Lypen, S., Wang, H. S., Cohen, I., Dixon, J. E., and McKinnon, D. (2001) *J. Physiol. (Lond)* **533,** 119–125
4. Kuo, H. C., Cheng, C. F., Clark, R. B., Lin, J. J., Lin, J. L., Hoshijima, M., Nguyen-Tran, V. T., Gu, Y., Ikeda, Y., Chu, P. H., Ross, J., Giles, W. R., and Chien, K. R. (2001) *Cell* **107,** 801–813
5. Morohashi, Y., Hatano, N., Ohya, S., Takikawa, R., Watabiki, T., Takasugi, N., Imaizumi, Y., Tomita, T., and Iwatsubo, T. (2002) *J. Biol. Chem.* **277,** 14965–14975
6. Shibata, R., Misonou, H., Campomanes, C. R., Anderson, A. E., Schrader, L. A., Doliveira, L. C., Carroll, K. I., Sweatt, J. D., Rhodes, K. J., and Trimmer, J. S. (2003) *J. Biol. Chem.* **278,** 36445–36454
7. Deschenes, I., and Tomaselli, G. F. (2002) *FEBS Lett.* **528,** 183–188
8. Dixon, J. E., Shi, W. M., Wang, H. S., McDonald, C., Yu, H., Wymore, R. S., Cohen, I. S., and McKinnon, D. (1996) *Circ. Res.* **79,** 659–668
9. Fiset, C., Clark, R. B., Shimoni, Y., and Giles, W. R. (1997) *J. Physiol. (Lond)* **500,** 51–64
10. Kaab, S., Dixon, J., Duc, J., Ashen, D., Nabauer, M., Beuckelmann, D. J., Steinbeck, G., McKinnon, D., and Tomaselli, G. F. (1998) *Circulation* **98,** 1383–1393
11. Brahmajothi, M. V., Campbell, D. L., Rasmusson, R. L., Morales, M. J., Trimmer, J. S., Nerbonne, J. M., and Strauss, H. C. (1999) *J. Gen. Physiol.* **113,** 581–600
12. Maletic-Savatic, M., Lenn, N. J., and Trimmer, J. S. (1995) *J. Neurosci.* **15,** 3840–3851
13. Hoffman, D. A., Magee, J. C., Colbert, C. M., and Johnston, D. (1997) *Nature* **387,** 869–875
14. Malin, S. A., and Nerbonne, J. M. (2001) *J. Neurosci.* **21,** 8004–8014
15. Burgoyne, R. D., and Weiss, J. L. (2001) *Biochem. J.* **353,** 1–12
16. Nakamura, T. Y., Pountney, D. J., Ozaita, A., Nandi, S., Ueda, S., Rudy, B., and Coetzee, W. A. (2001) *Proc. Natl. Acad. Sci. U. S. A.* **98,** 12808–12813
17. Guo, W., Malin, S. A., Johns, D. C., Jeromin, A., and Nerbonne, J. M. (2002) *J. Biol. Chem.* **277,** 26436–26443
18. Schrader, L. A., Anderson, A. E., Mayne, A., Pfaffinger, P. J., and Sweatt, J. D. (2002) *J. Neurosci.* **22,** 10123–10133
19. Jiang, Y. X., Lee, A., Chen, J. Y., Ruta, V., Cadene, M., Chait, B. T., and MacKinnon, R. (2003) *Nature* **423,** 33–41
20. Abbott, G. W., and Goldstein, S. A. N. (1998) *Quarterly Reviews Biophysics* **31,** 357–398
21. Sokolova, O., Kolmakova-Partensky, L., and Grigorieff, N. (2001) *Structure* **9,** 215–220
22. Sun, T., Naini, A. A., and Miller, C. (1994) *Biochemistry* **33,** 9992–9999
23. MacKinnon, R., and Miller, C. (1988) *J. Gen. Physiol.* **91,** 335–349
24. MacKinnon, R. (1991) *Nature* **350,** 232–235
25. Goldstein, S. A., and Miller, C. (1993) *Biophys. J.* **65,** 1613–1619
26. MacKinnon, R., and Miller, C. (1989) *Science* **245,** 1382–1385
27. Goldstein, S. A., Pheasant, D. J., and Miller, C. (1994) *Neuron* **12,** 1377–1388
28. Ranganathan, R., Lewis, J. H., and MacKinnon, R. (1996) *Neuron* **16,** 131–139
29. Goldstein, S. A., and Miller, C. (1992) *Biophys. J.* **62,** 5–7
30. Gross, A., Abramson, T., and MacKinnon, R. (1994) *Neuron* **13,** 961–966
31. Zhou, M., Morais-Cabral, J. H., Mann, S., and MacKinnon, R. (2001) *Nature* **411,** 657–661
32. Rhodes, K. J., Strassle, B. W., Monaghan, M. M., Bekele-Arcuri, Z., Matos,

[2] Kim, L. A., Furst, J., Gutierrez, D., Butler, M. H., Xu, S., Goldstein, S. A. N., and Grigorieff, N. (2004) *Neuron*, in press.

M. F., and Trimmer, J. S. (1997) *J. Neurosci.* **17,** 8246–8258
33. Gulbis, J. M., Zhou, M., Mann, S., and MacKinnon, R. (2000) *Science* **289,** 123–127
34. Knaus, H. G., Folander, K., Garcia, C. M., Garcia, M. L., Kaczorowski, G. J., Smith, M., and Swanson, R. (1994) *J. Biol. Chem.* **269,** 17274–17278
35. Ding, J. P., Li, Z. W., and Lingle, C. J. (1998) *Biophys. J.* **74,** 268–289
36. Inagaki, N., Gonoi, T., and Seino, S. (1997) *FEBS Lett.* **409,** 232–236
37. Clement, J. P. t., Kunjilwar, K., Gonzalez, G., Schwanstecher, M., Panten, U., Aguilar-Bryan, L., and Bryan, J. (1997) *Neuron* **18,** 827–838
38. Shyng, S., and Nichols, C. G. (1997) *J. Gen. Physiol.* **110,** 655–664
39. Wang, K. W., and Goldstein, S. A. N. (1995) *Neuron* **14,** 1303–1309
40. Chen, H., Kim, L. A., Rajan, S., Xu, S., and Goldstein, S. A. N. (2003) *Neuron* **40,** 15–23
41. Nadal, M. S., Ozaita, A., Amarillo, Y., de Miera, E. V.-S., Ma, Y., Mo, W., Goldberg, E. M., Misumi, Y., Ikehara, Y., Neubert, T. A., and Rudy, B. (2003) *Neuron* **37,** 449–461
42. Kreusch, A., Pfaffinger, P. J., Stevens, C. F., and Choe, S. (1998) *Nature* **392,** 945–948
43. Kobertz, W. R., Williams, C., and Miller, C. (2000) *Biochemistry* **39,** 10347–10352